

## ELASTIC LAND FULL-WAVEFORM INVERSION IN THE MIDDLE EAST: METHOD AND APPLICATIONS

O. Leblanc<sup>1</sup>, A. Sedova<sup>1</sup>, G. Lambaré<sup>1</sup>, T. Allemand<sup>1</sup>, O. Hermant<sup>1</sup>, D. Carotti<sup>1</sup>, D. Donno<sup>1</sup>, N. Masmoudi<sup>1</sup>

<sup>1</sup> CGG

### Summary

---

Applications of full-waveform inversion (FWI) to land data have proven much more challenging than to marine data. The difficulties are linked to a lower signal-to-noise ratio but also to a greater influence of elastic wave phenomena in these data sets, especially those characterized by strong elastic property contrasts. The Middle East, where FWI-dedicated acquisitions and pre-processing work-flows have been developed, has emerged as a promising proving ground for land acoustic FWI. But it also proved to be challenging due to strong elastic effects from alternating fast and slow velocity layers in the shallow section. Elastic land FWI then appears as a natural solution to be investigated, especially considering that it becomes more practical thanks to the progresses of the computing capacities. We study the potential of elastic land FWI to overcome the limitations of acoustic land FWI, through a set of synthetic and real data applications to typical challenging areas from the Middle East. We show the improved data fitting leading to an increased resolution and stability that can be obtained with elastic land FWI compared to acoustic land FWI when inverting diving waves. We also present some preliminary inversion results of ultra-low frequency surface-waves obtained by interferometry.

## Elastic land full-waveform inversion in the Middle East: method and applications

### Introduction

The application of acoustic FWI to land data (Mei et al., 2015; Wang et al., 2020; Vigh et al., 2021) has proven less successful than to marine data, despite the design of dedicated land acquisitions (Mahrooqi et al., 2012; Stopin et al., 2014). While a difficulty resides in the high noise level of land data, the presence of strong elastic property contrasts is a major limiting factor (Pérez Solano and Plessix, 2019). While dedicated land FWI workflows have been proposed to mitigate the acoustic approximation (Sedova et al., 2019; Hermant et al., 2020; Masclet et al., 2021), elastic FWI has also been investigated (Pérez Solano et al., 2013). While elastic FWI is not a new development (Crase et al., 1990), industrial adoption has lagged that of acoustic FWI because of the very high computing cost. It is now re-gaining traction thanks to its ability to retrieve an accurate velocity model where acoustic FWI fails (Pérez Solano and Plessix, 2019), especially in the Middle East, where shallow velocity profiles frequently consist of alternating fast and slow velocity layers with strong contrasts of elastic parameters. We present several applications of land elastic FWI to typical synthetic and real data sets from the Middle East. We highlight the critical components of the workflow (the free-surface boundary condition and diving-wave mute), compare elastic and acoustic FWI results, and show initial results from ultra-low frequency interferometrically derived shot gathers.

### Elastic land FWI

We have developed a 3D VTI elastic land FWI algorithm that inverts for  $V_p$ ,  $V_s$ ,  $\varepsilon$  models (density is derived from Gardner's relation). While the biggest change from an acoustic FWI algorithm is the elastic wave propagation, other challenges arise from the multi-parameter inversion, and the need for selecting or balancing the various data components entering the inversion (Adwani et al., 2021). Using a free-surface boundary condition is also critical. However, this generates high-energy surface waves that dominate the FWI process but provide very limited information on deep structures. To remedy this, a modified surface boundary

condition was proposed by Plessix and Pérez Solano (2015) to give modeled data dominated by body waves only. In Figure 1 we show the impact of the type of surface boundary condition (free-surface, modified and absorbing) on the far-offset diving-waves for a synthetic case study inspired by the geology of the south of the Sultanate of Oman (Figure 3). We observe the modified and absorbing boundary conditions differ significantly from the free-surface one apart from the first wave train. Hence, we decided to use the closest to the real world case, namely a free-surface boundary condition but to associate it with an inner mute, preventing any interference of the ground roll, even at low

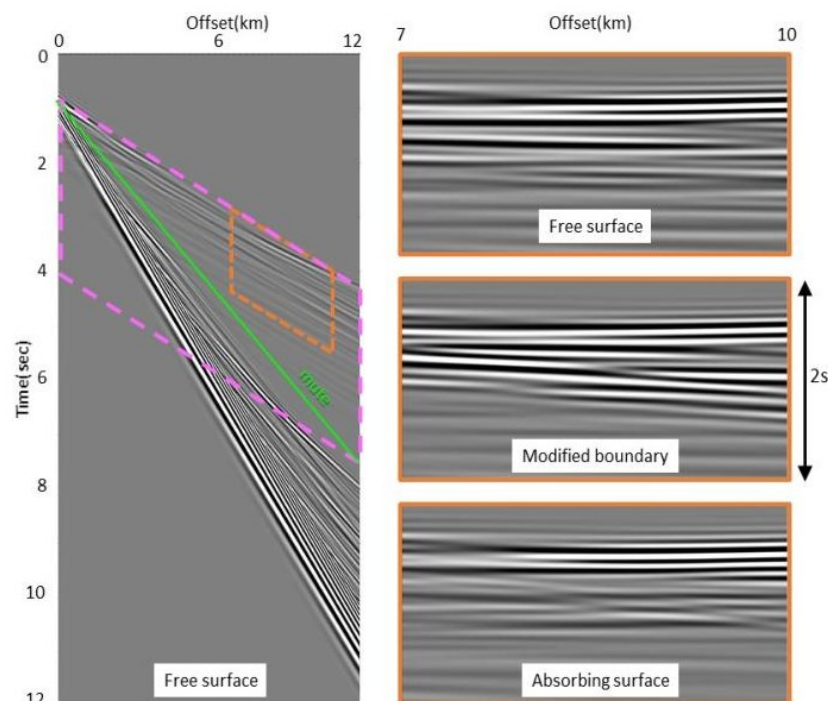
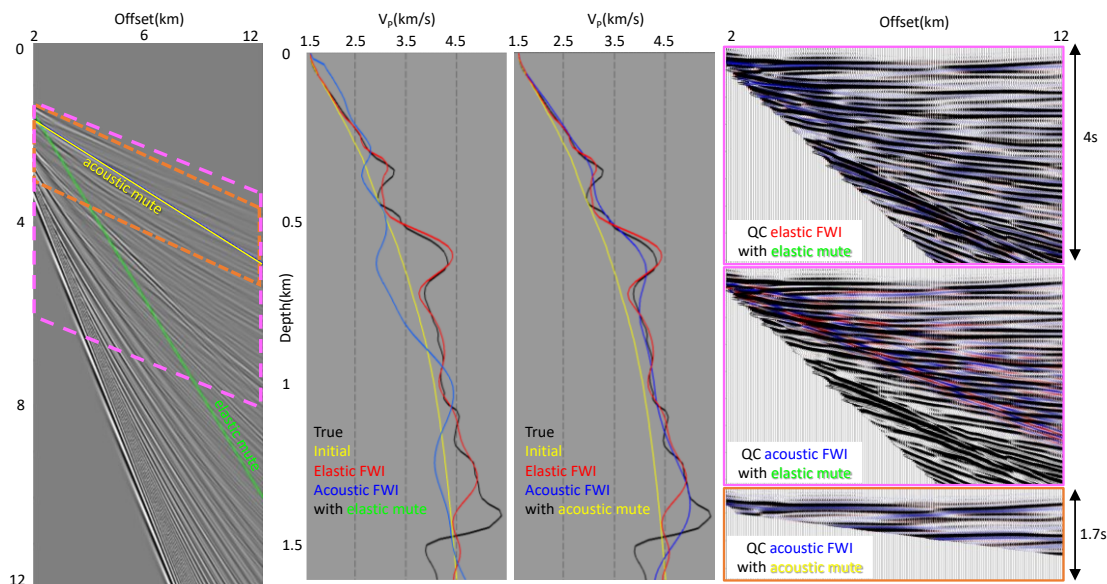


**Figure 1: Elastic full-wave modelling on the Oman synthetic model: Impact of surface boundary conditions on the far-offset diving-wave modelling. The data for various surface boundary conditions in the panels on the right are shown after linear moveout (for easier comparison) and located at the position of the orange box on the full shot record on the left.**

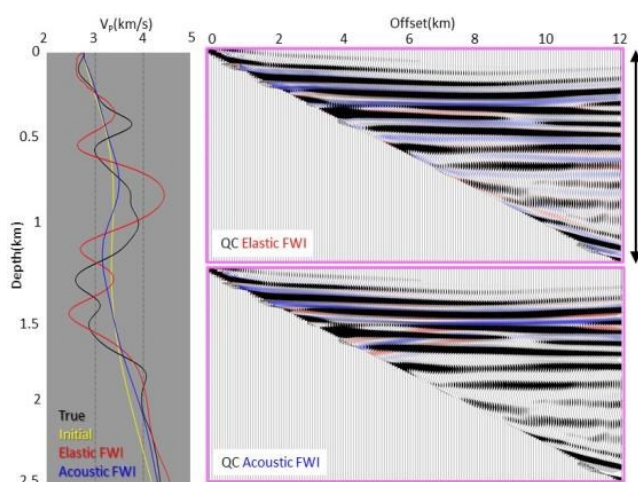
frequencies (the inner mute used for the Oman experiment is shown in Figure 1).

### Synthetic tests

We investigate the benefits of elastic land FWI on synthetic cases representative of the Middle East, with workflows leaning on recent developments in land FWI (Sedova et al., 2019; Pérez Solano and Plessix, 2019; Adwani et al., 2021). We designed two laterally invariant isotropic velocity profiles inspired from the geologies of north Kuwait (Bharti et al., 2016) and Oman (Pérez Solano and Plessix, 2019). Figures 2 and 3 show the  $V_P$  models as black curves.  $V_S$  is derived from a constant  $V_P/V_S$  ratio and density is constant. The maximum offset is 12 km, and the frequency band of the source signature



**Figure 2: Kuwait synthetic case.** Left) observed data, mutes and location of pink and orange boxes shown on the left. Middle)  $V_P$  profiles: true model, initial model and models inverted with acoustic and elastic FWI. Right) data fit QC: observed (wiggles) versus modeled data (blue/red) for the final 12 Hz elastic FWI model, and acoustic FWI models obtained with elastic and acoustic mutes.



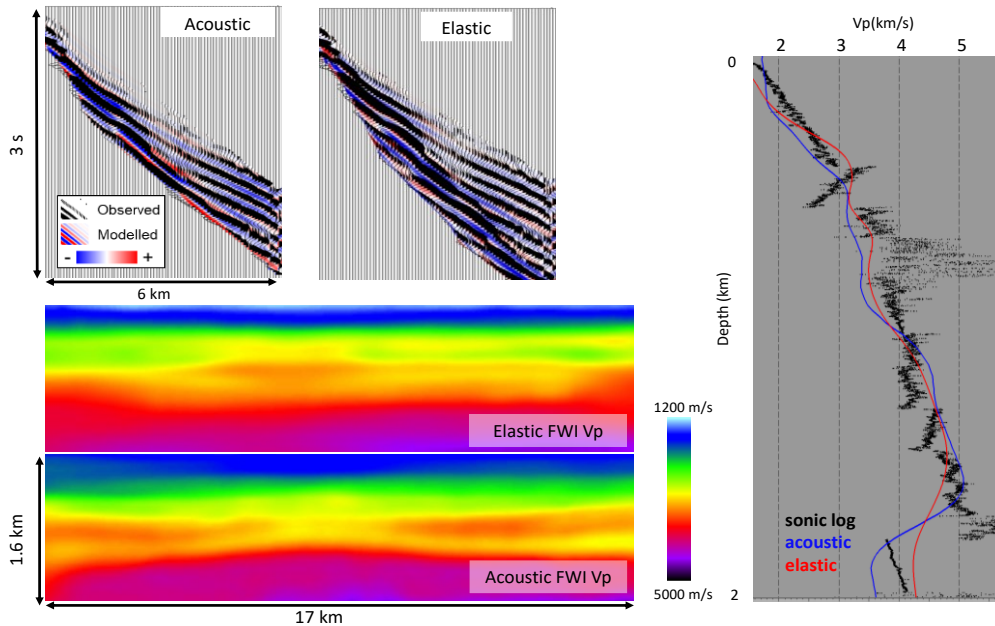
**Figure 3: Oman synthetic case:** Left)  $V_P$  profiles: true model, initial model and models obtained from acoustic and elastic FWI. Right) data fit QC: observed (wiggles) versus modeled data (blue/red) in the final FWI models at 4 Hz. The location of the panel, after linear moveout, is indicated by the pink box in Figure 1.

Figure 3 shows the more challenging Oman synthetic case study where OT FWI is done up to 4 Hz, similar to Pérez Solano and Plessix (2019). We observe an improved data fitting allowing to recover some elements of two major velocity inversions.

is [1.5, 12] Hz. For the comparison, the same elastic data and inner mute were used (emphasizing the far-offset diving waves) and the same initial velocity model. On the north Kuwait dataset, acoustic and elastic FWI were performed using a multi-scale approach from 2 Hz up to 12 Hz, using a combination of least-square and Optimal Transport FWI objective function (Messud et al., 2021). Figure 2 shows the resulting  $V_P$  velocity models and the associated data QC for the acoustic and elastic FWI. While elastic FWI converges towards the true model, the acoustic FWI could not converge when using the same inner mute as for the elastic FWI. A much tighter inner mute solved the issue, illustrating the fact that acoustic FWI can only describe the first diving-wave train. The use of elastic FWI ensures better robustness to the inner mute choice and improved data fitting leading to an increased resolution.

### Real data examples

The first data set was acquired in north Kuwait with a sweep starting at 2 Hz and a maximum offset of 9 km. The region is known for shallow velocity inversions that generate strong multiples. This geological context is particularly challenging for velocity model building, which then relies on complex sequences of FWI and tomography. The comparison of the results of elastic and acoustic FWI is shown in Figure 4. As in our synthetic experiment, the inversion used diving waves only. To allow acoustic FWI to converge towards a reasonable velocity model, we used a tighter inner mute. An improved resolution is obtained with elastic FWI, which recovers the velocity inversion at 400 m depth.



**Figure 4: Kuwait real case study:** Bottom left) velocity models: final 9 Hz VTI acoustic FWI (bottom), final 9 Hz VTI elastic FWI (top). Top left) data fit QC: observed (wiggle) versus modeled data (blue/red) from left to right: acoustic FWI and elastic FWI. Right)  $V_P$  velocity profiles inverted with acoustic FWI and elastic FWI, compared to a  $V_P$  sonic log.

The second data set from Oman consists of ultra-low frequency shot gathers reconstructed by 3D interferometry from continuous recording (Le Meur et al., 2020). Surface waves appear down to 0.3 Hz, far below the minimum frequency of the active sweep source (1.5 Hz for this study). Here the elastic FWI was used to invert the  $V_S$  model from the ultra-low frequency surface waves. Encouraging preliminary results are shown in Figure 5, indicating this could be a promising method to obtain an initial  $V_S$  background model (Adwani et al., 2021).

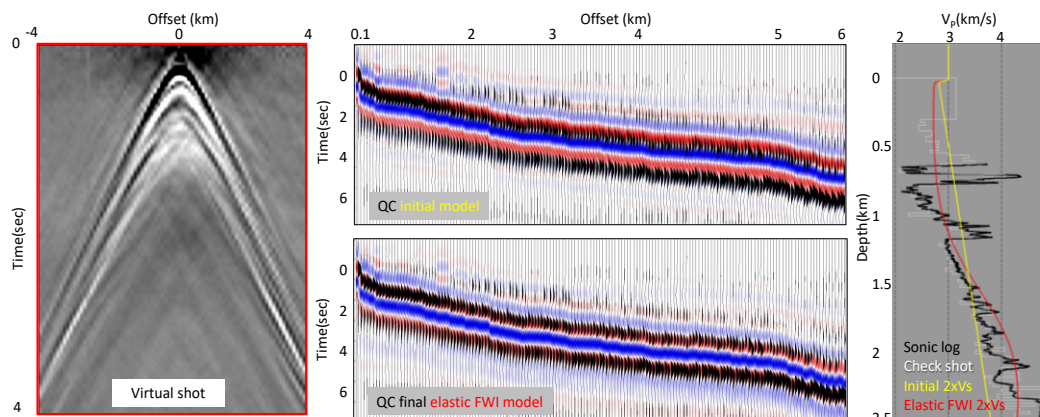


**Figure 5: Oman real data set:** Left) ultra-low frequency data obtained by interferometry. Middle) data fit QC: observed (wiggle) versus modeled data (blue/red) for initial and final elastic FWI models (inverted to 1 Hz). Right)  $V_S$  models converted to  $V_P$  and compared to  $V_P$  sonic log.

## Conclusion

In many areas of the Middle East, strong contrasts in elastic parameters make land FWI challenging for velocity model building. Complex workflows based on acoustic FWI have been developed with some success (Masclet et al., 2021), but elastic FWI is now feasible thanks to the ever increasing computing power and considerable processing experience. We have shown results obtained from both acoustic and elastic FWI, highlight the importance of the free-surface boundary condition and diving-wave mute, and illustrate some of the benefits of elastic FWI, such as improved output model fidelity.

## Acknowledgements

We thank Kuwait Oil Company and Petroleum Development Oman and the Ministry of Energy and Minerals of the Sultanate of Oman for the permission to use and publish the first and second real data examples, respectively. We also thank CGG for permission to publish this work.

## References

- Adwani, A., Danilouchkine, M., Plessix, R., Soni, A., Jahdhami, M., Abri, S., Ernst, F., Ten Kroode, F. [2021] Subsurface imaging with elastic FWI using surface and diving waves: 3D land data from south Oman. *83<sup>rd</sup> EAGE Conference & Exhibition*, Extended Abstracts.
- Bharti, S., Stopin, A., Pérez Solano, C. A., Plessix, R.-E., Lutz, J., Al-Qadeeri, B., Dashti, Q., Narhari, S., Olusegun, K. [2016] Application of an anisotropic elastic multiparameter waveform inversion on a land data set from north Kuwait. *86<sup>th</sup> Annual International Meeting*, Expanded Abstracts, 1201-1205.
- Cruse, E., Pica, A., Noble, M., McDonald, J., Tarantola, A. [1990] Robust elastic nonlinear waveform inversion: Application to real data. *Geophysics*, **55**(5), 527–538.
- Hermant, O., Aziz, A., Warzocha, S., Al Jahdhami, M. [2020] Imaging complex fault structures on-shore Oman using optimal transport full waveform inversion. *82<sup>nd</sup> EAGE Conference & Exhibition*, Extended Abstracts.
- Le Meur, D., Donno, D., Courbin, J., Solyga, D., Prescott, A. [2020] Retrieving ultra-low frequency surface waves from land blended continuous recording data. *90<sup>th</sup> SEG International Meeting*, Expanded Abstracts, 1855-1859.
- Mahrooqi, S., Rawahi, S., Yarubi, S., Abri, S., Yahyai, A., Jahdhami, M., Hunt, K., Shorter, J. [2012] Land seismic low frequencies: Acquisition, processing and full wave inversion of 1.5–86 Hz. *82<sup>nd</sup> SEG International Meeting*, Expanded Abstracts.
- Masclet, S., Bouquard, G., Prigent, H. [2021] Multi-wave and full-waveform inversion in Southern Oman. *83<sup>rd</sup> EAGE Conference & Exhibition*, Extended Abstracts.
- Mei, J., Ahmed, S., Searle, A., Ting, C.-O. [2015] A practical acoustic full waveform inversion workflow applied to a 3D land dynamite survey. *85<sup>th</sup> SEG International Meeting*, Expanded Abstracts, 1220–1224.
- Messud, J., Carotti, D., Hermant, O., Sedova, A., Lambaré, G. [2021] Optimal transport full-waveform inversion: from theory to industrial applications with examples from the Sultanate of Oman. *First Break*, **39**(12), 45 – 53.
- Pérez Solano, C. A., Stopin, A., Plessix, R.-E. [2013] Synthetic study of elastic effects on acoustic full waveform inversion. *75<sup>th</sup> EAGE Conference & Exhibition*, Extended Abstracts, Th P10 10.
- Pérez Solano, C. A., Plessix, R.-E. [2019] Velocity-model building with enhanced shallow resolution using elastic waveform inversion - An example from onshore Oman. *Geophysics*, **84**(6), R977–R988.
- Plessix, R.-E., Pérez Solano, C. A. [2015] Modified surface boundary conditions for elastic waveform inversion of low-frequency wide-angle active land seismic data. *Geophysical Journal International*, **201**(3), 1324–1334.
- Sedova, A., Royle, G., Allemand, T., Lambaré G., Hermant, O. [2019] High-frequency acoustic land full-waveform inversion: a case study from the Sultanate of Oman. *First Break*, **37**(1), 75-81.
- Stopin, A., Plessix, R.-E., Al Abri, S. [2014] Multiparameter waveform inversion of a large wide azimuth low-frequency land data set in Oman. *Geophysics*, **79**(3), WA67-WA77.
- Vigh, D., Cheng, X., Xu, Z., Jiao, K. [2021] Land full Waveform Inversion Application from Topography. *83<sup>rd</sup> EAGE Conference & Exhibition*, Extended Abstracts.
- Wang, D., Chen, C., Zhuang, D., Mei, J., Wang, P. [2020] Land FWI: Challenges and Possibilities. *82<sup>nd</sup> EAGE Conference & Exhibition*, Extended Abstracts.